

Charge and spin ordering in $\text{La}_{2-x}\text{Sr}_x\text{NiO}_{4.00}$ with $x = 0.135$ and 0.20

V. Sachan and D. J. Buttrey

Department of Chemical Engineering, University of Delaware, Newark, Delaware 19716

J. M. Tranquada, J. E. Lorenzo, and G. Shirane

Physics Department, Brookhaven National Laboratory, Upton, New York 11973

(Received 24 October 1994)

We report neutron-scattering experiments that reveal coupled incommensurate peaks arising from magnetic as well as charge ordering at low temperatures ($T \leq 100$ K) in stoichiometric $\text{La}_{2-x}\text{Sr}_x\text{NiO}_{4+\delta}$ ($\delta=0.00$) crystals. In contrast with the long-range ordering of holes and spins observed recently in $\text{La}_2\text{NiO}_{4.125}$, the correlations are short ranged in Sr-doped La_2NiO_4 and the incommensurability ϵ is 0.25 and 0.12 for $x=0.20$ and 0.135, respectively. Based on our study and previous reports on $\text{La}_{2-x}\text{Sr}_x\text{NiO}_{4+\delta}$, the modulation wave vector appears to be a sensitive function of net hole concentration, $p = x + 2\delta$. The magnetic correlation length increases with doping and the incommensurability follows the simple relationship $\epsilon \approx p$.

With the discovery of high- T_c superconductivity in layered cuprates, there has been intense interest in the structure and properties of K_2NiF_4 -structured oxides. Compositions which alter the in-plane hole concentration by heterovalent metal substitution (A site) and/or by incorporation of oxygen defects as interstitials or vacancies are of interest for understanding factors influencing electronic localization and magnetic correlations. In the prototypical compound La_2CuO_4 , the antiferromagnetic insulator phase is rapidly destroyed by doping,¹ leading to a metallic superconducting phase at moderate hole concentrations. In contrast, La_2NiO_4 remains insulating up to fairly high dopant concentrations. In particular, long-range antiferromagnetic order survives up to $\delta \lesssim 0.11$ in $\text{La}_2\text{NiO}_{4+\delta}$.^{2,3} At $\delta=0.125$, evidence of a combined ordering of Ni spins and dopant-induced holes has been observed.⁴ It appears that the holes collect in domain walls between antiferromagnetic stripes.

The results of several studies on Sr-doped La_2NiO_4 suggest that a qualitatively similar ordering of holes and spins may occur in this system. The first evidence was the observation at low temperature of broad incommensurate magnetic peaks in a single-crystal neutron-scattering study of $\text{La}_{1.8}\text{Sr}_{0.2}\text{NiO}_{4+\delta}$, with $\delta \approx -0.04$.⁵ More recently, an electron-diffraction study of ceramic samples of $\text{La}_{2-x}\text{Sr}_x\text{NiO}_{4+\delta}$ with $x \geq 0.2$, prepared under oxidizing conditions, revealed structural modulations that were attributed to polaron ordering.⁶ A relationship between the modulation wave vector of the structural distortion and that associated with the magnetic peaks found in the earlier neutron study was discussed; however, that proposed relationship is quite different from the harmonic structure observed in $\text{La}_2\text{NiO}_{4.125}$. A resolution of this conflict is possible when one considers the net hole concentration p of the different samples, where $p = x + 2\delta$. Recent thermogravimetric studies have shown that the value of δ in Sr-doped crystals is quite sensitive to the atmosphere in which a sample is

prepared.⁷ Thus, samples with the same value of x but annealed in atmospheres with quite different oxygen partial pressures, as in the neutron- and electron-diffraction studies mentioned above, will have substantially different hole concentrations.

In the present paper we report a neutron-scattering study of Sr-substituted crystals with $x=0.135$ and 0.20 for which the oxygen content is stoichiometric, i.e., $\delta=0.00$, so that we have $p=x$. When the $x=0.20$ sample is cooled below ~ 100 K, we observe extra peaks centered at $(1 \pm \epsilon, 0, l)$, for integer l , and $(4 - 2\epsilon, 0, l)$, with l odd. The value of ϵ is almost exactly $\frac{1}{4}$. The first-harmonic peaks are associated with magnetic scattering, as in the earlier study by Hayden *et al.*⁵ (although ϵ differs), while the second-harmonic peaks are attributed to atomic displacements associated with charge ordering, as in the electron-diffraction study by Chen, Cheong, and Cooper.⁶ However, the relationship between the spin and charge ordering wave vectors is exactly the same as that observed in $\text{La}_2\text{NiO}_{4.125}$.⁴ For the $x=0.135$ sample, only the first-harmonic peaks are observed, with a width comparable to their separation, and $\epsilon \approx 0.12$.

The single crystals were grown by radio-frequency induction skull melting as described elsewhere.⁸ Oxygen stoichiometry variations were investigated by thermogravimetric analysis as a function of annealing T and P_{O_2} .⁷ These thermogravimetric data were used to select annealing conditions which will produce very nearly stoichiometric compositions, i.e., for which the intrinsic oxygen sublattices are complete, with an insignificant net concentration of intercalated oxygen. The $x=0.135$ specimen was annealed at 1100°C in high-purity argon with residual oxygen content $\log_{10} P_{\text{O}_2} (\text{atm}) \approx -4.5$ to provide $\delta=0.002(2)$. Using the same conditions the $x=0.20$ crystal has $\delta=0.000(2)$. Note that δ will not be measurably altered during the quench since the atmosphere provides insufficient available oxygen. This has

been confirmed by comparison with iodometric determinations on similar samples. Note that the $x=0.20$ crystal studied by Hayden *et al.*⁵ was annealed at 1000°C with $\log_{10}P_{\text{O}_2}(\text{atm})=-11.7$, for which our thermogravimetric data are consistent with their reported value of $\delta \approx -0.04$. Chen, Cheong, and Cooper⁶ prepared their powder specimens in air [$\log_{10}P_{\text{O}_2}(\text{atm})=-0.7$] or 200 bar O_2 [$\log_{10}P_{\text{O}_2}(\text{atm})=+2.3$] at $T=850^\circ\text{C}$, conditions which should induce a substantial level of oxygen excess ($\delta \gg +0.02$) for $x \approx 0.2$ based on extrapolation of our thermogravimetric results to superambient pressures.

Neutron-scattering experiments on these crystals were performed on the H4M ($x=0.135$) and H8 ($x=0.20$) triple-axis spectrometers at the High Flux Beam Reactor at Brookhaven National Laboratory. The incident neutron wavelength was 2.35 \AA ($E_i=14.7 \text{ meV}$), with pyrolytic graphite filters employed before and after the sample to suppress higher-order contamination. Horizontal collimations of $40'-20'-40'-80'$ were used for the $x=0.135$ sample and $40'-40'-40'-40'$ for the $x=0.20$ sample. The crystals were aligned, mounted in an Al can filled with He exchange gas, and cooled inside a Displex closed-cycle He refrigerator. Along with three-axis elastic scans, some two-axis measurements were also made. The two-axis scans were performed using the special geometry that allows one to effectively integrate over the fluctuations of a two-dimensional antiferromagnet while scanning the in-plane momentum transfer.⁹⁻¹¹ In keeping with the crystallographic notation used in earlier experiments with pure and Sr-doped La_2NiO_4 , indexing will be done on the $\sqrt{2}\mathbf{a} \times \sqrt{2}\mathbf{b} \times \mathbf{c}$ K_2NiF_4 supercell. Each crystal was initially aligned in the $(h\ 0\ l)$ zone, and the $x=0.20$ sample was further investigated in the $(h\ k\ 0)$ zone.

Both crystals are orthorhombic at low temperature. In the $x=0.135$ case, the tetragonal-to-orthorhombic transition temperature T_S is 230 K , and at $T=10 \text{ K}$, $a=5.431 \text{ \AA}$, $b=5.457 \text{ \AA}$, and $c=12.590 \text{ \AA}$. For $x=0.20$ the orthorhombic splitting was too small to measure; however, superstructure reflections associated with octahedral tilting appear below $T_S \approx 70 \text{ K}$; lattice constants at 10 K are $a \approx b \approx 5.429 \text{ \AA}$ and $c=12.635 \text{ \AA}$. These transition temperatures are remarkably similar to $\text{La}_{2-x}\text{Sr}_x\text{CuO}_4$ (Refs. 1 and 12) with matching values of x .

Scans of several of the superstructure reflections that are found at 10 K in the $x=0.20$ crystal are presented in Fig. 1. Magnetic peaks occur at $(h \pm \epsilon, 0, l)$ with h odd and $\epsilon \approx \frac{1}{4}$. [In contrast, the magnetic Bragg peaks corresponding to the commensurately ordered antiferromagnetic state in undoped La_2NiO_4 appear at $(h, 0, l)$ with h odd and l integer.] Figure 1(a) shows that the $(1 \pm \epsilon, 0, l)$ peaks are relatively sharp when scanned along h ; however, a scan along $(1 - \epsilon, 0, l)$ [Fig. 1(b)] shows very broad structure. The width of the peaks in Fig. 1(a) indicate a static in-plane correlation of $\sim 40 \text{ \AA}$. By analogy with the structures observed in $\text{La}_2\text{NiO}_{4.125}$,⁴ we expect to find peaks associated with a structural modulation at $(h \pm 2\epsilon, 0, l)$ with h even and l odd. Scans through the $(4 - 2\epsilon, 0, l)$ peak are shown in Figs. 1(c) and (d). Although the peak is weak, it is well defined. The finite peak width in the scan along l demonstrates that short-range correlations exist between NiO_2 layers. Looking back at Fig. 1(b), the modulated intensity along l found for the magnetic peaks is consistent with broad, overlapping peaks centered at integer values of l , where the peaks at odd l are stronger than those at even l .

The relationship between the ϵ and 2ϵ peaks can be further characterized by the temperature dependences of

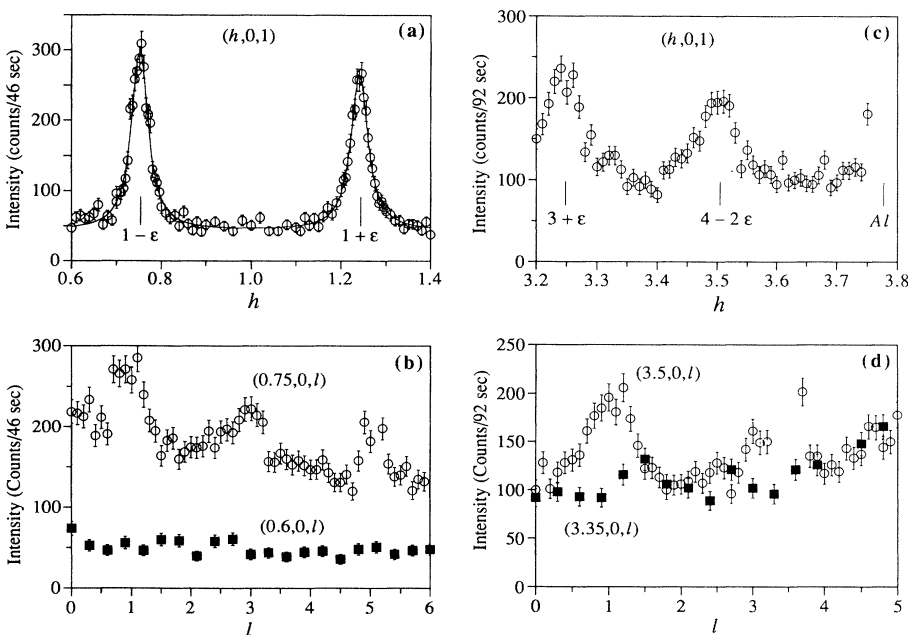


FIG. 1. Scans of elastic scattering through representative magnetic and structural superlattice peaks for the $x=0.20$ crystal at 10 K . (a) Scan through magnetic peaks along $(h, 0, 1)$. (b) Scan of the $(1 - \epsilon, 0, l)$ peak along l . Solid squares indicate background measured along $(0.6, 0, l)$. (c) Scan along h through the structural-modulation peak at $(4 - 2\epsilon, 0, l)$. (d) Scan through the same peak along l . Solid squares indicate background measured along $(3.35, 0, l)$.

their intensities, which are presented in Fig. 2(a). With increasing temperature, the heights of both types of peaks decrease gradually. The 2ϵ peaks appear to survive to higher temperatures; however, if we consider the intensity obtained in the energy-integrated (two-axis) measurements of the magnetic scattering, the magnetic correlations appear to track the behavior of the 2ϵ peak rather closely. Figure 2(b) shows that the peak widths start to increase well before the peak heights approach zero. The temperature dependence indicates a freezing of short-range correlations, in contrast to the long-range order that develops in $\text{La}_2\text{NiO}_{4.125}$.⁴

To explain the superlattice peaks observed below 110 K in $\text{La}_2\text{NiO}_{4.125}$ we proposed a model⁴ in which stripes of holes alternate with stripes of antiferromagnetically ordered Ni spins. The hole stripes, which should occur at a spacing of $2a$ for $p = 2\delta = 0.25$, act as antiphase boundaries for the magnetic domains,¹³ so that the magnetic repeat distance is $4a$. The resulting value of ϵ is $\frac{1}{4}$, just the same as we observe in the $x = 0.20$ crystal. For the oxygen-doped crystal it was also possible to determine the spin orientation from measurements in the $(h k 0)$ zone. Magnetic peaks were observed at the positions $(1 \pm \epsilon, 0, 0)$ and $(1, \pm \epsilon, 0)$. The intensities of the latter pair of peaks were less than 10% of the former, consistent with spins pointing transverse to the modulation wave vector. In contrast, the two sets of peaks have essentially equal intensities for the $x = 0.20$ sample. The simplest model to explain this involves a spiral spin structure; the

difference from the oxygen-doped case is surprising, but might be related to the lack of long-range order. Concerning the short-range correlations in the $x = 0.20$ crystal, the width of the magnetic peaks in the $(h k 0)$ zone are found to be isotropic, in contrast to the anisotropic peak widths reported by Hayden *et al.*⁵

To see how the correlations vary with the level of doping, it is interesting to consider the results for the $x = 0.135$ crystal. Elastic scans through the two-dimensional (2D) magnetic peak position are shown in Fig. 3(a). The very broad peak observed at 10 K is gone at 80 K; the inset shows that the transition temperature is ~ 65 K. At 10 K the scattered intensity varies weakly (except for multiple-scattering peaks) as one scans along $(1, 0, l)$, indicating that the static correlations are essentially two dimensional. Magnetic correlations can still be observed above 65 K by integrating over dynamical fluctuations. Figure 3(b) shows a two-axis scan through the 2D magnetic scattering at 100 K. It appears that the two-axis data can be described by a pair of very broad incommensurate peaks. The fit indicated by the solid curve yields $\epsilon = 0.12(1)$; the width corresponds to an instantaneous correlation length of ~ 10 Å. The fact that the spins appear to have short-range incommensurate correlations suggest that the holes may be localized in domain walls as for $x = 0.20$, although we have not observed any 2ϵ peaks in this crystal.

We have summarized some of our results in Fig. 4. The open circles mark the structural transition temperatures observed in our two Sr-doped crystals, and, for comparison, the solid line indicates the phase boundary

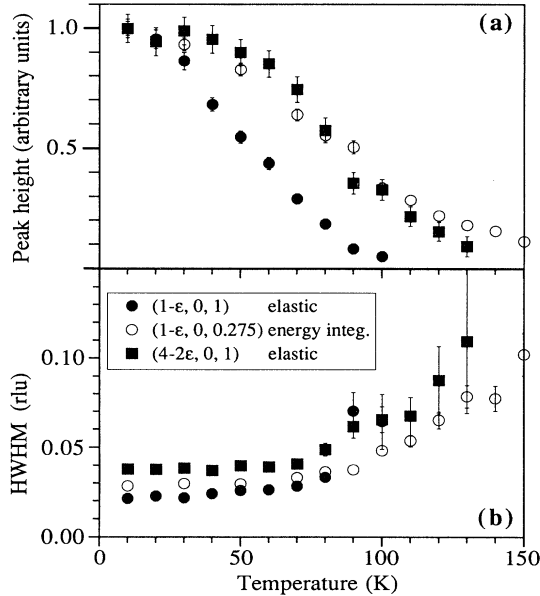


FIG. 2. Temperature dependence of peak heights (a) and widths (b) (HWHM = half width at half maximum) for $x = 0.20$. Peak heights are normalized to values at 10 K. Widths are measured in reciprocal-lattice units (rlu). Solid symbols indicate results from elastic scans along h through the $(1-\epsilon, 0, 1)$ peak (circles) and the $(4-2\epsilon, 0, 1)$ peak (squares). Open circles correspond to energy-integrated two-axis scans through $(0.75, 0, 0.275)$.

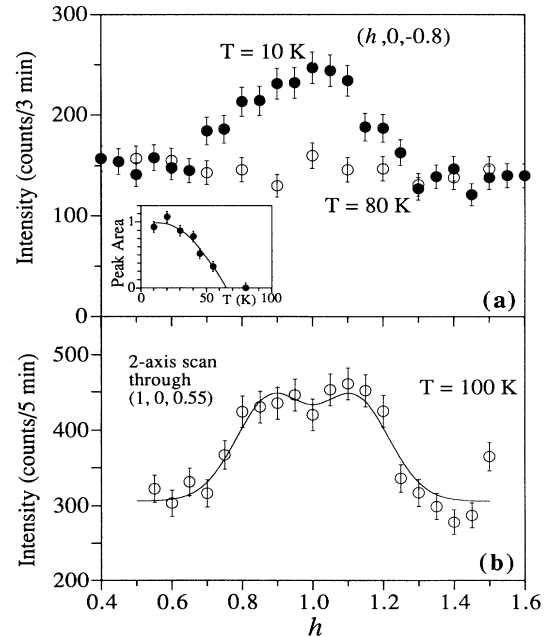


FIG. 3. Scans through the 2D antiferromagnetic scattering rod at $(1, 0, l)$ for the $x = 0.135$ crystal. (a) Elastic scans along $(h, 0, -0.8)$ at 10 and 80 K. Inset shows temperature dependence of the peak area. (b) Energy-integrated two-axis scan through $(1, 0, 0.55)$ at 100 K. Solid line is a fit of two symmetrically displaced Gaussian peaks.

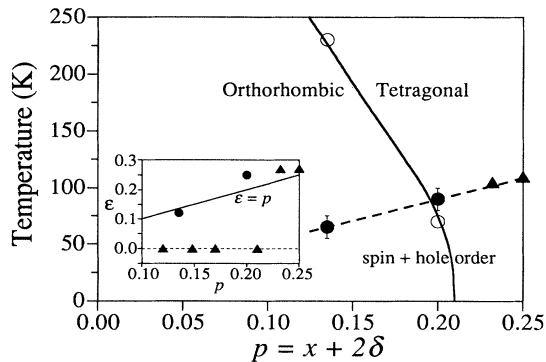


FIG. 4. Partial summary of transition temperatures for $\text{La}_{2-x}\text{Sr}_x\text{NiO}_{4.00}$ and $\text{La}_2\text{NiO}_{4+\delta}$ (Ref. 4) plotted as a function of the nominal hole concentration, $p = x + 2\delta$. Open circles: structural transitions for Sr-doped crystals. Solid line: structural phase boundary for $\text{La}_{2-x}\text{Sr}_x\text{CuO}_4$ (Refs. 1 and 12). Solid circles: magnetic freezing transition for Sr-doped crystals. Solid triangles: transition temperatures for spin and charge ordering in O-doped crystals. Dashed line is a guide to the eye. Inset: Incommensurability ϵ as a function of p for Sr-doped (circles) and O-doped (triangles) crystals. Solid line corresponds to $\epsilon \approx p$.

reported^{12,1} for $\text{La}_{2-x}\text{Sr}_x\text{CuO}_4$. The filled circles represent the temperatures at which the static incommensurate magnetic correlations appear, while the solid triangles indicate the transition temperatures for spin and charge order observed in $\text{La}_2\text{NiO}_{4+\delta}$.^{2,4} The properties of the two systems show a similar trend in ordering temperature when plotted as a function of the nominal hole concentration, p . The inset shows that the trend in the incommensurability with doping is described approximately by $\epsilon \approx p$.

A trend that is not included in the figure concerns the magnetic correlation length, which we find *increases* with doping. This result is in stark contrast to the conclusion of Hayden *et al.*⁵ who found that the correlation length in their crystal was comparable to the mean spacing of Sr dopants. The precise role of the randomly distributed Sr dopants in limiting the correlation length is not yet clear. The long-range order observed in $\text{La}_2\text{NiO}_{4+\delta}$ (Refs. 2 and 4) occurs in the presence of both ordered dopants and a higher hole concentration.

Continuing the comparison with the results of Hayden *et al.*,⁵ we note that they observed an incommensurability $\epsilon \approx 0.16$. Using their values of $x = 0.20$ and $\delta \approx -0.04$, the corresponding hole concentration is $p \approx 0.12$. These quantities are roughly consistent with

the trend $\epsilon \approx p$.

To compare with the results of Chen, Cheong, and Cooper,⁶ we must first discuss a difference in the indexing of peak positions. They indexed the charge-ordering superlattice peaks with respect to antiferromagnetic reciprocal-lattice points, rather than regular reciprocal-lattice points. Their incommensurate splitting parameter δ (not to be confused with our symbol for oxygen excess) is related to ϵ by the formula $2\epsilon = 1 - \delta$. Now, for $0.2 \leq x \leq 0.4$ they observed superlattice peaks characterized by $\delta \approx \frac{1}{3}$, which corresponds to $\epsilon \approx \frac{1}{3}$. Cheong *et al.*¹⁴ suggested that this modulation is associated with $p = \frac{1}{3}$. Again, this result is consistent with the trend $\epsilon \approx p$. The fact that superlattice peaks with $\epsilon \approx \frac{1}{3}$ were observed in samples with $x = 0.2$ (Ref. 6) would also be consistent if the samples have a substantial oxygen excess, as one might expect from the conditions of sample preparation (annealing at 850°C under 200 bars of oxygen pressure). On the other hand, the direct comparison by Chen *et al.*⁶ of the electron-diffraction results on an oxygenated $x = 0.2$ ceramic sample with the neutron-scattering results of Hayden *et al.* on an oxygen-deficient crystal clearly seems inappropriate.

For completeness, we note that an intriguing study of diffuse x-ray scattering in a single crystal of $\text{La}_{1.8}\text{Sr}_{0.2}\text{NiO}_{4+\delta}$ was recently reported by Isaacs *et al.*¹⁵ They observed diffuse streaks in the neighborhood of (001) peaks, the intensity of which increased substantially as the temperature was raised from 10 to 300 K. Any simple connection between those observations and the present work is not apparent to us.

In conclusion, our neutron-scattering study has provided direct evidence for the combined ordering of spins and holes in $\text{La}_{2-x}\text{Sr}_x\text{NiO}_{4.00}$. Although the correlations are only short range, the nature of the order appears to be qualitatively similar to that observed previously in $\text{La}_2\text{NiO}_{4.125}$.⁴ A comparison of the two systems indicates that the proper parameter for characterizing the periodicity of the ordering and the transition temperature is the net hole concentration, $p = x + 2\delta$. This result underlines the importance of characterizing the concentrations of both substitutional dopants and excess oxygen in studies of doping effects in transition-metal oxide systems.

Work at Brookhaven was carried out under Contract No. DE-AC02-76CH00016, Division of Materials Sciences, U.S. Department of Energy. V.S. and D.J.B. acknowledge support from the National Science Foundation under Contract No. DMR-8914080.

¹R. J. Birgeneau and G. Shirane, in *The Physical Properties of High Temperature Superconductors*, edited by D.M. Ginsberg (World Scientific, Singapore, 1989).

²K. Yamada, T. Omata, K. Nakajima, Y. Endoh, and S. Hosoya, *Physica C* **221**, 355 (1994).

³J. M. Tranquada, Y. Kong, J. E. Lorenzo, D. J. Buttrey, and V. Sachan, *Phys. Rev. B* **50**, 6340 (1994).

⁴J. M. Tranquada, D. J. Buttrey, V. Sachan, and J. E. Lorenzo,

Phys. Rev. Lett. **73**, 1003 (1994).

⁵S. M. Hayden, G. H. Lander, J. Zaretsky, P. J. Brown, C. Stassis, P. Metcalf, and J. M. Honig, *Phys. Rev. Lett.* **68**, 1061 (1992).

⁶H. Chen, S-W. Cheong, and A. S. Cooper, *Phys. Rev. Lett.* **71**, 2461 (1993).

⁷V. Sachan and D. J. Buttrey (unpublished).

⁸D. J. Buttrey, H. R. Harrison, J. M. Honig, and R. R. Schart-

- man, J. *Solid State Chem.* **54**, 407 (1984).
- ⁹G. Aeppli and D. J. Buttrey, *Phys. Rev. Lett.* **61**, 203 (1988).
- ¹⁰R. J. Birgeneau, J. Skalyo, Jr., and G. Shirane, *Phys. Rev. B* **3**, 1736 (1971).
- ¹¹G. Shirane, Y. Endoh, R. J. Birgeneau, M. A. Kastner, Y. Hidaka, M. Oda, M. Suzuki, and T. Murakami, *Phys. Rev. Lett.* **59**, 1613 (1987).
- ¹²H. Takagi, R. J. Cava, M. Marezio, B. Batlogg, J. J. Krajewski, W. F. Peck, Jr., P. Bordet, and D. E. Cox, *Phys. Rev. Lett.* **68**, 3777 (1992).
- ¹³The first use of a magnetic antiphase domain model (without the hole domain walls) to explain the positions and widths of the incommensurate magnetic peaks in $\text{La}_{1.8}\text{Sr}_{0.2}\text{NiO}_4$ was by P. J. Brown, S. M. Hayden, G. H. Lander, J. Zaretsky, C. Stassis, P. Metcalf, and J. M. Honig, *Physica B* **180&181**, 380 (1992).
- ¹⁴S-W. Cheong, H. Y. Hwang, C. H. Chen, B. Batlogg, L. W. Rupp, Jr., and S. A. Carter, *Phys. Rev. B* **49**, 7088 (1994).
- ¹⁵E. D. Isaacs, G. Aeppli, P. Zschack, S-W. Cheong, H. Williams, and D. J. Buttrey, *Phys. Rev. Lett.* **72**, 3421 (1994).